

Investigations of non-circular turning using a high-acceleration drive unit based on aerostatic bearing principle

Benjamin Clauß¹, Stephan Schaller², Andreas Schubert¹

¹Chemnitz University of Technology, Professorship Micromanufacturing Technology, Reichenhainer Str. 70, 09126 Chemnitz, Germany

²AeroLas GmbH, Grimmerweg 6, 82008 Unterhaching, Germany

Corresponding author: benjamin.clauss@mb.tu-chemnitz.de

Abstract

Non-circular part geometries are typically of high relevance for powertrain components and in the field of joining without additional fastening elements. Typically, expensive special-purpose machine tools are necessary to generate or finish these geometries. The machinery represents a high investment risk combined with low flexibility in job order production.

A prototypical drive unit is developed to complement existing machine tools and to reduce investment, yet providing non-circular machining capabilities. A machining technology based on non-circular turning allows for a simple kinematics, but requires a higher kinematic performance of the drive unit. Experimental investigations based on eccentrics, P3G, and cam profiles are used to investigate the machining capabilities of the developed drive unit. The examinations address a steel grade of the type 42CrMo4 in a quenched and tempered state and in a hardened state. As cutting materials cemented carbide and cubic boron nitride (CBN) are used depending on the heat treatment of the material. Different tool geometries with corner radii of 0.4 mm or 0.8 mm and tools with a wiper geometry are applied.

The results indicate an appropriate geometrical accuracy for the investigated eccentrics and P3G profiles. However, there are still challenges with regard to accuracy of the cam profiles. The application of an increased corner radius and a wiper geometry in the form of a trailing edge allow for reduced surface roughness values.

The presented research enhances the exploitation of non-circular turning in job order production. As the necessary drive unit is intended to complement existing lathes, the investment risk for potential users can be limited.

Accuracy, Drive, Surface, Turning

1 Introduction

For non-circular turning there is a given state of the art addressing superimposition of highly dynamic movements to conventional turning processes. High-performance drive units typically incorporate piezoelectric actuators, linear motors, or voice coils.

Zhou, Henson, and Wang apply a complementary drive unit with a machine tool for non-circular machining of pistons. A linear motor generates the additional motion. Drive unit and machine tool are interlinked via a RS232 interface and a digital signal processor [1].

Ma, Hu, and Zhang propose the application of a piezoelectric drive unit. In order to achieve a long-travelling system maintaining a high movement frequency and precision, a flexure hinge structure is introduced. The solid state hinge design incorporates two piezoelectric actuators combined with a lever system to amplify the actuator travel [2].

Beekhuis et al. address the non-circular turning of bearing rings to compensate clamping force induced form deviations. After applying the clamping load, the resulting workpiece contour is determined using a stylus measuring setup. Eventually, the workpiece is machined using a vertical lathe combined with a fast tool servo (FTS). The integrated tool holder connected to the FTS via a flexure hinge allows for a maximum tool travel of up to 300 μm [3].

Ma, Tian, and Hu focus on the development of a FTS for non-circular machining. The drive system combines a piezoelectric actuator and a flexure hinge to amplify the actuator travel. In experimental investigations a maximum displacement of the FTS

of up to 442 μm and a repetitive accuracy of 2 μm are determined [4].

Kim, Li, and Tsao discuss the control design of a linear actuator for non-circular machining. The drive system intends to overcome limitations of FTSs in terms of a limited travel. The system is designed as a combination of electrohydraulic and piezoelectric actuators. The electrohydraulic component allows for rough positioning in a range of up to 25 mm. Precise motions up to 40 μm are realised with the piezoelectric stage [5].

Kim and Tsao also focus on the dynamic adaptation of the rake angle in non-circular turning. The superimposition of a linear motion in non-circular machining leads to alternating effective rake angles due to the changing curvature of the contour. The researchers combine a primary drive unit for the translatory motion with a linkage and an additional drive unit to dynamically adapt the rake angle throughout machining [6].

Morimoto et al. address the development of a drive system and the tool layout to generate non-circular free-form surfaces. The drive unit is based on a linear motor superimposing the required translatory motion. The tool path is calculated using a developed computer aided manufacturing (CAM) tool processing 3D workpiece and tool data [7].

Morimoto et al. also address optimisations of the introduced drive unit. For an acceleration of about 12 g, the slider is re-designed incorporating two linear motor driven tables. The tables consist of carbon fibre reinforced plastics (CFRPs) being powered by separate linear motors. Both tables are arranged in a tandem configuration [8].

Liu et al. investigate the combination of a voice coil motor (VCM) and a piezoelectric actuator to realise a flexure hinge based FTS. Strokes in a range of ± 0.5 mm are realised [9].

Scheiding et al. apply a VCM-driven FTS for free-form ultraprecision machining. With maximum strokes in the range of ± 3 mm microlense structures can be transferred to a hemispherical geometry with surface qualities < 4 nm [10].

2 Material and methods

2.1 Steel grade and heat treatment

The experimental investigations address a CrMo-alloyed heat-treatable steel of the type 42CrMo4 with applications in automotive and aerospace. The material is characterised by a comparably high ultimate tensile strength in the range of 900 MPa to 1200 MPa depending on the heat treatment. A high toughness is represented by a fracture elongation in the range of 10 % to 14 %. The heat treatments address quenching and tempering in addition to hardening.

2.2 Cutting material and tool geometry

Different cutting materials and tool geometries are applied depending on the heat treatment of the specimen material.

In turning of the quenched and tempered steel, cemented carbide indexable inserts are used as cutting material (Mitsubishi UE6020). The inserts are CVD-coated with several layers comprising Ti, Al_2O_3 , and TiCN. Standardised geometries of the type CCMT 09T304 and CCMT 09T308 are used to investigate the influence of different corner radii of 0.4 mm and 0.8 mm. The inserts provide a clearance angle $\alpha_0 = 7^\circ$, chip breakers, an effective rake angle $\gamma_0 > 0^\circ$, and a tool included angle $\epsilon_r = 80^\circ$. Combined with a tool holder a tool cutting edge angle $\kappa_r' = 5^\circ$ results.

In machining of the hardened steel, CBN-tipped indexable inserts are used with the CBN grade BNC200 as cutting material (Sumitomo Electric). The cutting material is characterised by a proportion of 65 % to 70 % CBN particles with an average size of 4 μ m, bound in a TiN matrix. The substrate is coated with a ceramic TiAlN/TiCN-layer of an average thickness of 2 μ m. Indexable inserts with the standardised geometry CCGW 09T304 are used exhibiting a corner radius of 0.4 mm. Additionally, inserts of the type CCGW 09T304-WG2 with a 0.4 mm corner radius and a trailing minor cutting edge are used. The CBN-tipped tools do not provide chip breakers. Accordingly, the tool angles are identical to the indexable inserts for the machining of the quenched and tempered steel except for the effective rake angle $\gamma_0 = 0^\circ$.

Table 1. Process parameters applied throughout the cutting tests.

Shape	Tool	n (min ⁻¹)	f (mm)	a_p (mm)
Ecc.	CCMT 09T304	710	0.1	0.2
	CCMT 09T308			
P3G	CCGW 09T304			
Cam	CCGW 09T304-WG2			0.1

2.3 Cutting conditions and experimental setup

The experimental setup for the cutting tests applies the combination of a machine tool of the type SPINNER PD 32 combined with a prototypical high-performance drive unit. The drive unit incorporates the active parts of two linear motors actuating a single lightweight design slider. The CNC of the machine tool and the control unit of the drive system are separate entities. While the CNC controls the rotational speed and the feed motion, the drive unit motion is controlled independently. However, the superimposed linear motion is synchronised based on a rotary en-

coder signal throughout each spindle rotation. The slider features an interface to mount a tool holder which is capable of carrying standard geometry indexable inserts. For non-circular turning a comparably high clearance angle is required to prevent collisions between the flank face of the tool and the generated surface. As the used standard geometry indexable inserts provide clearance angles of about 7° , an additional 8° inclination is included within the tool holder. The drive unit is mounted above the spindle axis to enable sufficient clearance for positioning and feed motions. The drive unit design is based on aerostatic bearing principle. An operational pressure of about 0.5 MPa and an internal water cooling enable permanent accelerations of up to 350 m/s². The control loop uses the spindle angle phi for path synchronisation and generates the control commands for both linear motors. Figure 1 illustrates the experimental setup consisting of the lathe and the drive unit, the structural design, and the control loop design.

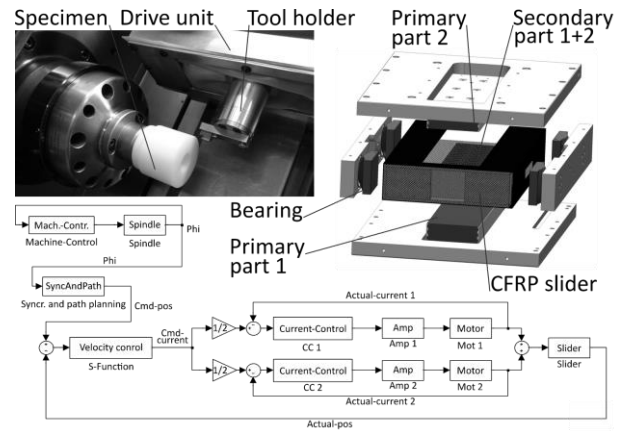


Figure 1. Experimental setup, structural design, and control loop design of the applied high-acceleration drive unit.

The specimen geometry is represented by cylindrical sections with a tool relief towards the mandrel. The outer diameter of the specimens is pre-machined to an initial value of 54.5 mm. For pre-machining the drive unit is used without superimposing an additional motion. Subsequently, the non-circular geometry is produced in consecutive paths, incrementally positioning the drive unit towards the rotational axis of the specimen. The machined length is defined with 15 mm. With each path, the machined length is incrementally reduced down to a final value of 10 mm in order to prevent circumferential contact of the tool corner at the end of each path. Thereby, the tendency of vibration generation can be reduced significantly. In the cutting experiments, eccentrics, P3G, and cam profiles are generated for different heat treatments of the steel. Regarding the cutting conditions, the spindle speed is kept unchanged at a value of 710 min⁻¹ representing a maximum cutting speed v_c of about 107 m/min. The feed f is defined with a value of 0.1 mm. The depth of cut a_p is adapted depending on the heat treatment of the steel. While the quenched and tempered material is machined with an a_p -value of 0.2 mm, for the hardened steel a depth of cut of 0.1 mm is applied. All experiments are conducted without cooling lubricant. Table 1 summarises the process parameters and the applied cutting tool geometries.

2.4 Evaluation of accuracy and surface properties

For the evaluation of the addressed non-circular geometries different quantitative and qualitative methods are used. Firstly, the surface structure is taken into consideration. On the one hand, three tactile roughness measurements for each surface are used to quantify the surface profile. The primary profiles are measured using an instrument of the type Mahr LD 120, a traversed length of 5.6 mm, and an evaluated length of 4 mm. The

separation of the waviness and the roughness profiles is achieved by applying a filter with a cut-off wavelength λ_c of 0.8 mm. Using the roughness profiles, the surface roughness depth R_z is determined.

On the other hand, 3D surface plots of the generated surfaces are realised based on point cloud data acquired by laser scanning microscopy with an instrument of the type Keyence VK-9700. The surface data are acquired for a measuring field of 1 mm \times 1 mm. The processing comprises pruning the data to the required measuring field dimensions, levelling using a subtraction method, and removing the convex basic shape of the specimens. Accordingly, the surface plots represent the acquired surfaces without additional filtering.

For the evaluation of size and form deviations, coordinate measurements are realised for each profile with a measuring machine of the type Carl Zeiss Prismo 7. In this context, the machined non-circular geometries are assessed in comparison to the target geometries extracted from the control unit.

3 Results and discussion

The experimental investigations primarily are focused on two main criteria regarding the generated non-circular geometries. Firstly, the geometrical accuracy is evaluated using the coordinate measurements. In order to quantify possible deviations, the specified target geometries for each of the addressed profiles are used as a reference. Subsequently, a tolerance band is predetermined with reference to the target geometry and a range of ± 0.05 mm. Secondly, the surface structure is taken into consideration. In addition to roughness evaluations, 3D surface representations allow for a qualitative assessment of the generated surfaces.

3.1 Geometrical accuracy

Figure 2 presents the results of the coordinate measurements for two cutting tests addressing a polygonal contour defined by a maximum stroke of 3.6 mm and a nominal size of 50 mm according to standard DIN 32711-1 [11]. The results are obtained by the application of comparable tool geometries with a corner radius of 0.4 mm. However, the polygonal profiles are realised using the same specimen material in quenched and tempered (QT) and in hardened (H) condition. Accordingly, cemented carbide and CBN are applied as cutting materials. For the machining operations in hardened state, the depth of cut is limited to 0.1 mm to prevent an overloading of the drive unit in terms of the resulting force components.

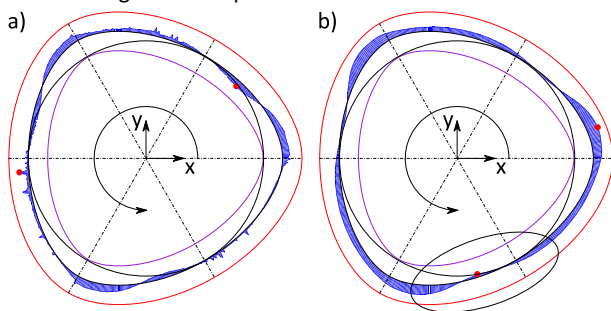


Figure 2. Form accuracy when machining a polygonal (P3G) profile using 42CrMo4 in a) Quenched and tempered and b) Hardened condition (CCxx 09T304, $n = 710 \text{ min}^{-1}$, $f = 0.1 \text{ mm}$, $a_p = 0.2 \text{ mm}$ (QT), $a_p = 0.1 \text{ mm}$ (H)), red line – upper limit, black line – target geometry, violet line – lower limit, blue bars – form deviations.

The findings indicate a comparable behaviour of the drive system when machining the quenched and tempered and the hardened specimen material. The most significant deviations from the predefined target geometries can be seen in the areas before and behind the local stroke maxima. The focused polygonal profile is characterised by three local maxima, leading to a

repetition of the motion patterns after an increment of 120° . The geometrical deviations approximately start at the tangential contact points between the polygonal contour and the inherent maximum inscribed diameter (please see marker Figure 2b). The generation of the final geometry is achieved by several tool paths. In this context, for the final path producing the generated surface the drive unit is positioned to the smallest overall radius of the non-circular contour. When focusing on the sections, in which one of the local maxima is located, it can be seen, that the drive unit moves behind the ideal geometry leading to a positive form deviation before crossing the target contour and producing lower measures than intended. Subsequently, there is a counter reaction by the drive system control leading to positive deviations again towards the next local maximum. Moreover, it can be seen, that certain scatter effects appear when machining the quenched and tempered steel. This is attributed to a significantly higher toughness of the material leading to an increased vibration tendency and a higher tool load. The maximum deviation from the ideal geometry amounts up to about 0.04 mm when machining the quenched and tempered material and about 0.035 mm for the hardened steel.

Figure 3 presents the results of the coordinate measurements for the addressed cam profile. Comparable to the presented polygonal profile, the targeted geometry is realised using the 42CrMo4 steel with both heat treatments. In order to maintain comparability, the presented results are based on an identical tool geometry with a corner radius of 0.4 mm in both cases.

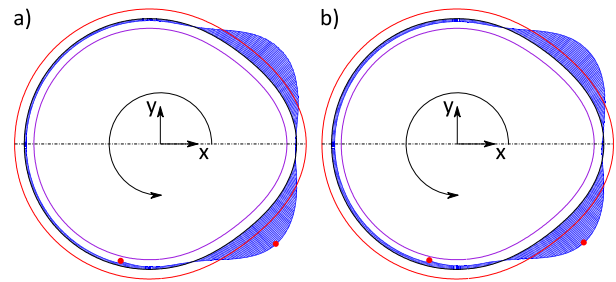


Figure 3. Form accuracy when machining a cam profile using 42CrMo4 in a) Quenched and tempered and b) Hardened condition (CCxx 09T304, $n = 710 \text{ min}^{-1}$, $f = 0.1 \text{ mm}$, $a_p = 0.2 \text{ mm}$ (QT), $a_p = 0.1 \text{ mm}$ (H)).

In contrast to the polygonal profile, the cam geometry is characterised by only one local maximum with a slightly higher stroke of 4 mm per workpiece revolution. Referring to Figure 3 the maximum is localised within the angular range from 270° to 90° , while there is no stroke motion for the remaining angular range producing the base circle of the cam contour. It becomes clear that the most significant deviations can be found in the sections before and behind the stroke maximum. In both cases positive deviations can be found, meaning that there is oversize compared to the targeted geometry. Referring to the machining process, the non-circular profiles are generated with the drive unit mounted above the spindle axis as shown in Figure 1. Accordingly, the specimens are rotating clockwise with the given rotational speed throughout the machining process. While the deviations before the stroke maximum indicate a premature motion of the drive system, after passing the local peak the system appears unable to follow the contour quickly enough. As the dynamic requirements, in terms of tool travel per time unit, are lower compared to the generation of the polygonal profile it is assumed that the deviations can not be attributed to dynamic limitations of the drive unit. It appears more reasonable that there are further developments needed in terms of the drive system control. At this point there is a maximum deviation of 0.18 mm compared to the specified geometry when machining the specimen material in both heat treatments.

3.2 Surface roughness and structure

Figure 4 shows a 3D surface representation of generated surfaces for the cam profile. In the illustrated cases both specimens are machined in the hardened state using CBN-tipped indexable inserts. In order to investigate the potentials of a modified tool geometry, a tool with a corner radius of 0.4 mm and a tool with a trailing edge combined with a corner radius of 0.4 mm are applied. The process parameters are kept unchanged in order to maintain comparability.

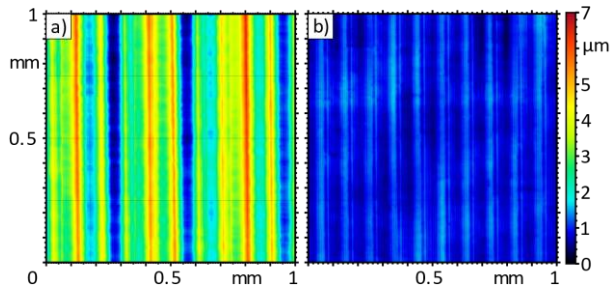


Figure 4. Surface structure when machining a cam profile using 42CrMo4 in hardened state with different tool geometries a) CCGW 09T304 with corner radius and b) CCGW 09T304-WG2 with wiper geometry ($n = 710 \text{ min}^{-1}$, $f = 0.1 \text{ mm}$, $a_p = 0.1 \text{ mm}$).

The findings indicate a significant reduction of the surface roughness values combined with a more uniform surface structure when using a wiper geometry. This is attributed to the trailing edge embodying a significantly increased corner radius thus leading to a lower kinematic roughness component within the surface structure. Quantitatively, the wiper edge allows for R_z values of about $1.1 \mu\text{m} \pm 0.1 \mu\text{m}$ with rather low fluctuations compared to $4.2 \mu\text{m} \pm 1.2 \mu\text{m}$ when using a 0.4 mm corner radius. The application of a wiper edge apparently enables a stabilisation of the process due to an increased contact length, leading to evenly pronounced feed marks. However, there are complex interactions between the heat treatment state of the specimens, the applied cutting material, the cutting edge conditions, and the corner geometry. Throughout the machining of eccentrics, the application of a trailing edge benefited the appearance of vibrations. The achieved roughness values increased significantly, although the influence of dynamic effects resulting from the superimposed stroke motion is lower.

Figure 5 presents the surface structure when machining eccentrics in quenched and tempered steel. Cemented carbide inserts with corner radii of 0.4 mm and 0.8 mm are applied for the generation of the illustrated surfaces.

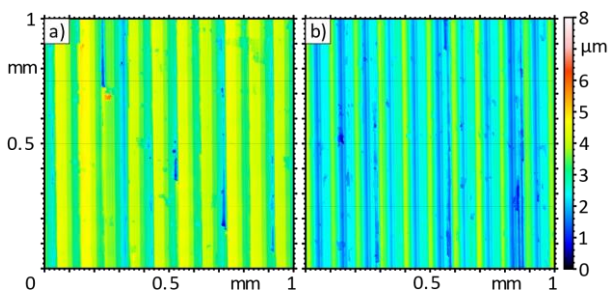


Figure 5. Surface structure when machining an eccentric using 42CrMo4 in quenched and tempered state applying different tool geometries with a) CCMT 09T304 with a corner radius of 0.4 mm and b) CCMT 09T308 with a corner radius of 0.8 mm ($n = 710 \text{ min}^{-1}$, $f = 0.1 \text{ mm}$, $a_p = 0.2 \text{ mm}$).

As it can be seen in Figure 5, the non-circular turning of the quenched and tempered material provides different surface characteristics compared to the hardened material. In general, higher roughness values occur. Machining of the eccentric geometry applying a corner radius of 0.4 mm leads to R_z -values of $5.1 \mu\text{m} \pm 0.5 \mu\text{m}$. When using an increased corner radius of

0.8 mm, the resulting roughness can be reduced to values of $3.7 \mu\text{m} \pm 0.4 \mu\text{m}$ with a slightly lower fluctuation. The 3D embodiments verify that the ridges and valleys of the feed marks are pronounced less evenly on the generated surfaces for the quenched and tempered compared to the hardened steel. This is attributed to the higher toughness, negatively affecting tool-workpiece-interaction and process stability.

4 Summary and conclusions

The results are obtained from experimental investigations of a non-circular turning process. In this context, a lathe is complemented with an additional prototypical drive unit based on aerostatic bearing principle. The high-acceleration drive provides a maximum permanent acceleration of 350 m/s^2 and allows for the generation of non-circular geometries such as eccentrics, polygonal P3G, and cam profiles. The cutting tests specifically address a steel grade of the type 42CrMo4 in quenched and tempered and in hardened condition.

The findings indicate that a high geometrical accuracy is achieved when machining eccentrics and polygonal profiles. In these cases, a narrow tolerance range of less than 0.05 mm is achieved. Currently, there are still challenges with reference to the machining of cam profiles. Regarding the target geometry before and behind the stroke maximum there are still inaccuracies exceeding the defined tolerances. Ongoing research should address these deficiencies optimising the control systems.

Acknowledgement

Supported by:



on the basis of a decision by the German Bundestag

This project was funded by the Federal Ministry for Economic Affairs and Energy, following a decision of the German Bundestag.

References

- [1] Zhou H, Henson B and Wang X 2005 Extracted control approach for CNC non-circular turning *Asian Journal of Control* **7**(1) 50-5
- [2] Ma H, Hu D and Zhang K 2005 A fast tool feeding mechanism using piezoelectric actuators in noncircular turning *Int. J. Adv. Manuf. Technol.* **27** 254-9
- [3] Beekhuis B L T, Brinksmeier E, Garbrecht M and Sölter J 2009 Improving the shape quality of bearing ring in soft running by using a fast tool servo *Prod. Eng. Res. Devel.* **3** 469-74
- [4] Ma H, Tian J and Hu D 2013 Development of a fast tool servo in noncircular turning and its control *Mechanical Systems and Signal Processing* **41** 705-13
- [5] Kim B-S, Li J and Tsao T-C 2004 Two-parameter robust repetitive control with application to a novel dual-stage actuator for noncircular machining *IEEE/ASME Transactions on Mechatronics* **9**(4) 644-52
- [6] Kim B-S and Tsao T-C 2010 Development of a novel variable rake angle mechanism for noncircular turning and its control *Journal of Mechanical Science and Technology* **24**(5) 1035-40
- [7] Morimoto Y, Emoto S, Moriyama T, Kato H, Nakagaki K, Suzuki N, Kaneko Y and Isobe M 2012 Creation of curved surface by lathe turning -Development of CAM system using original tool layout- *Procedia CIRP* vol 1 p 114-9
- [8] Morimoto Y, Moriyama T, Emoto S, Saito H, Nakagaki K, Kaneko Y and Isobe M 2012 Development of linear-motor-driven NC table for high-speed machining of 3D surface by lathe turning *Procedia CIRP* **1** 271-6
- [9] Liu Q, Zhou X, Xu P, Zou Q and Lin C 2012 A flexure-based long-stroke fast tool servo for diamond turning *Int. J. Adv. Manuf. Technol.* **59** 859-67
- [10] Scheiding S, Yi A Y, Gebhardt A, Li L, Risse S, Eberhardt R and Tünnermann A 2011 Freeform manufacturing of a microoptical lens array on a steep curved substrate by use of a voice coil fast tool servo *Optics Express* **19** 23938-51
- [11] DIN 32711-1, Shaft to collar connection – Polygon profile P3G – Part 1: Generalities and geometry (DIN 32711-1:2009-03)